Astron. Astrophys. 319, 867–880 (1997)

ASTRONOMY AND ASTROPHYSICS

Search for forced oscillations in binaries

I. The eclipsing and spectroscopic binary V 436 Persei ≡ 1 Persei⋆,⋆⋆

P. Harmanec[1], **P. Hadrava**[1], **S. Yang**[2], **D. Holmgren**[1], **P. North**[3], **P. Koubský**[1], **J. Kubát**[1], **and E. Poretti**[4]

[1] Astronomický ústav Akademie věd České republiky, 251 65 Ondřejov, Czech Republic (hec(had, david, koubsky, kubat)@sunstel.asu.cas.cz)
[2] Department of Physics and Astronomy, University of Victoria, P.O. Box 3055, Victoria, B.C., V8W 3P6, Canada (yang@uvastro.phys.uvic.ca)
[3] Institut d'Astronomie de l'Université de Lausanne, CH-1290 Chavannes-des-Bois, Switzerland (Pierre.North@obs.unige.ch)
[4] Osservatorio Astronomico, Via E. Bianchi 46, I-22055 Merate (CO), Italy (poretti@merate.mi.astro.it)

Received 20 May 1996 / Accepted 21 August 1996

Abstract. Outline of a project aimed at testing the presence of rapid line-profile variations in the atmospheres of hot components of close binaries is presented and its first results are described. An analysis of new electronic spectra of the eclipsing binary V436 Per from three observatories and of photoelectric observations, obtained earlier by several authors, leads to a unique determination of all basic physical elements of this interesting object. The first practical application of a new method of spectral disentangling allowed us to obtain, for the first time, individual accurate line profiles of both binary components and to derive their rotational velocities and orbital radial-velocity curves. We also detected absorption sub-features travelling from blue to red accross the He I 6678 line profile, in a series of six spectra taken during one night. At least one of the components of V436 Per is, therefore, a new hot line-profile variable.

Key words: stars: binaries: eclipsing – stars: binaries: spectroscopic – stars: fundamental parameters – stars: oscillations – stars: individual: V436 Per ≡ 1 Per

1. Introduction

One of the topical problems in the current research of early-type stars is to find cause(s) for and to understand the nature of rapid line-profile changes observed for many hot stars.

Historically, the line-profile variations were first recognized for a small group of sharp-lined early B stars, now known under the class name β Cep stars (see, e.g., Lesh and Aizenman 1978, Osaki 1986, Sterken and Jerzykiewicz 1993). Introduction of stable electronic spectral detectors in the seventies brought a real revolution to the subject. Smith (1977, 1978) discovered variable line asymmetries for several sharp-lined OB stars while Walker, Yang and Fahlman (1979) were the first to recognize another type of variation, now known as 'travelling sub-features' or 'moving bumps': small profile disturbances which gradually move (most often from blue to red) across the line profiles. Baade (1983) explicitly pointed out that both line-asymmetry changes and travelling sub-features do occur in the spectra of the same stars, and that they may be manifestations of one physical variation related to velocity fields in the stellar atmospheres. Further development of the subject will not be reviewed here. Readers are referred to ample existing literature on the subject, for example Jaschek and Groth (1982), Smith (1986), Slettebak and Snow (1987), Harmanec (1989), Baade (1991), Balona et al. (1994) and Štefl et al. (1995), among many others.

In brief, the competing interpretations include corotating surface or circumstellar structures, free non-radial oscillations, and *forced* non-radial oscillations in binary systems. It is the last hypothesis which will be considered here.

Speculations about the crucial role of duplicity for either triggering or at least modifying stellar pulsations are not new. Fitch (1967, 1969) called attention to the fact that many known β Cep stars are spectroscopic binaries and demonstrated, on particular examples, that the tide-raising potential does indeed affect the pulsations. A binary hypothesis of the β Cep phenomenon was presented at the end of sixties by Stothers and Simon (1969, 1970) who argued that the β Cep stars are the former secondaries of massive systems which underwent large-scale mass exchange between the binary components. This hypothesis was invalidated through the criticisms by Smak (1970), Plavec (1971), Percy and Madore (1971) and Lesh and Aizenman (1973). Among other arguments, these critics point to the lack of any evidence of duplicity for some particular and well-observed β Cep stars, to strong evidence that some of those β Cep stars which are found in binaries have clearly unevolved secondaries and to statistical findings that the binary frequency

Send offprint requests to: P. Harmanec

⋆ This research is based on spectra from the Dominion Astrophysical, Ondřejov, and Haute Provence Observatories

⋆⋆ Table 3 is only available in electronic form at CDS via anonymous ftp 130.79.128.5 or via http:/cdsweb.u-strasbg.fr/Abstract.html

Table 1. Journal of RV observations

Source	Epoch (JD−2400000)	No. of obs.	Dispersion (Å/mm)
1	19055.7–19409.7	4	?
2	19662.7–20828.6	59	40
3	20016.8	1	30
4	20369.9–21092.8	8	33
5	24042.9–30043.6	4	30
	30732.6–30733.6	2	51
6	35794.6–35833.6	16	34
7	49327.3–50114.3	14	17.2
8	49371.3	1	8.5
9	49744.6–50140.7	24	10.0
10	50056.9–50057.0	6	10.0

Details on sources of data and instruments used: 1 ...Abt (1970): Mt. Wilson 1.5-m reflector, prism spg.; 2 ...Beardsley (1969): Allegheny 0.79-m Keeler Memorial reflector, 1-prism Mellon spg.; 3 ...Frost et al. (1926): Yerkes 1.02-m refractor, Bruce 1-prism spg.; 4 ...Cannon (1918): Ottawa, 1-prism spg.; 5 ...Pearce & Petrie (1951): Dominion Astrophysical Observatory 1.83-m reflector, 1-prism spg.; 6 ...Blaauw & van Albada (1963): McDonald 2.08-m reflector, coudé grating spg.; 7 ...this paper: Ondřejov 2.0-m reflector, coudé grating spg. with a Reticon RL 1872F/30 detector with 15 μm pixels; 8 ...this paper: OHP 1.52-m reflector, Aurélie coudé grating spg. with a TH 7832 detector with 13 μm pixels; 9 ...this paper: DAO 1.22-m reflector, coudé grating spg. with a thick Loral 4096 $\times$ 200 CCD device with 15 μm pixels; 10 ...this paper: DAO 1.83-m reflector, Cassegrain grating spg. with a thick Loral 4096 $\times$ 200 CCD device with 15 μm pixels;

of β Cep stars is comparable to that of normal A stars. In a recent careful study, Pigulski & Boratyn (1992) failed to confirm the existence of a 10.9-d binary companion to β Cep itself, reported earlier by Fitch (1969), and their conclusion was fully supported by Aerts et al. (1994) who analyzed an excellent series of electronic spectra of β Cep and found no night-to-night RV variations larger than 1 km s^{-1} (after they removed the short period RV changes). Osaki (1971) pointed out that slow periodic changes of the mean (γ) value of the β Cep radial-velocity (RV hereafter) curve need not always be due to orbital motion in a binary system but may also be caused by a superposition of two oscillations with similar periods. He suggested this as an explanation for Fitch's (1969) result for β Cep. Pigulski & Boratyn (1992) demonstrated, however, that the secular changes in the main pulsational period of β Cep are caused by light time effect as the star moves in orbit with a distant binary companion, discovered by speckle interferometry. On the other hand, an archetype line-profile variable ε Per (HD 24760) was found to be a 14.1-d spectroscopic binary in an eccentric orbit (Harmanec 1989, Harmanec & Tarasov 1990, Tarasov et al. 1995). Recently, Chapellier et al. (1995) published an interesting study of the well-known β Cep star EN Lac (16 Lac, HD 216916) which is also an eclipsing binary. They found that the amplitude of the longest of the three short periods of light and RV variations, known for years for this star ($0^{\rm d}.169$, $0^{\rm d}.171$, and $0^{\rm d}.182$), varies with the phase of the orbital period (or rotational period of the primary).

Kato (1974) investigated the conditions under which nonradial oscillations could either be excited or become multiperiodic due to a resonant interaction with the tidal mode in binary systems. Waelkens and Rufener (1983) made a *photometric* search for the presence of β Cep oscillations in 17 binaries with hot primary components falling into the range of β Cep instability strip. They concluded that such oscillations are obviously damped by tidal interactions since they were unable to find them in any of the 11 binaries with orbital periods shorter than 4 d. This empirical result may perhaps be related to the theoretical work of Tassoul (1987, 1988) who proposed an efficient hydrodynamical mechanism of orbital synchonization and circularization of binaries. Effects of dynamic tides treated as forced oscillations and their effects on free oscillations was also investigated by Polfleit and Smeyers (1990). Lee (1993) studied the angular momentum transfer by tidally forced oscillations in massive binaries. He argued that a Be-type disk could be created as a consequence of an outflow caused by resonant coupling between the tidal and a free oscillation.

Considering all these developments, we feel that the question regarding the true role of duplicity on at least some of the rapid line-profile and light variables deserves further study.

2. Project SEFONO: search for forced oscillations in binaries

Project SEFONO (acronym for SEarch for FOrced Nonradial Oscillations) which we have launched represents a new approach to the problem. Since it is almost impossible to rule out duplicity of any given star beyond doubt, we decided to attack the problem from another direction. Let us postulate, as an initial working hypothesis, that the periodic variations of the gravitational potential from the binary companion, caused either by the motion in an eccentric orbit or by the lack of synchronism between the primary's rotation and binary revolution, represent a sufficient condition to excite and maintain observed short-period pulsations in the OBA primary. If so, then any O, B or A star, which is a component of a binary system with non-circular orbit or with non-synchronous rotation (and an orbital period shorter than some, as yet unknown, limit) should pulsate. The idea, therefore, is to observe systematically the known shorter-periodic binaries with O, B, and A primaries and to test them for the presence of rapid line-profile changes. While the spectroscopic search for line-profile variations is certainly much more time-comsuming than photometric surveys, its main advantage is a greater sensitivity to high-order oscillations which often do not produce observable photometric effects. It is well-known that the travelling sub-features remain detectable in the spectra of Spica, which no longer exhibits detectable β Cep light oscillations (Walker et al. 1982).

Completion of such a project should allow us to confirm, refute or modify the above hypothesis. It is conceivable, for

Table 2. Journal of photoelectric observations

Source	Epoch (JD−2400000)	No. of obs.	Passband(s)	Comparison	Check
Güssow (1929)	24473.5–25279.3	15	*blue*	4 Per	
	25125.5–25234.4	5	*blue*	2 Per	
Kurtz (1977)	42706.7–42744.7	91	y	HR 540	HR 502
North et al. (1981); this paper	37190.5–44626.4	190	*Geneva* 7C	all sky	–
Percy (1982)	44555.7–44925.7	26	b	HR 540	–
Poretti (1982); this paper	44919.3–45000.4	102	V	HR 540	4 Per
Böhme (1984)	45638.3–45780.3	19	V	HR 540	–
Poretti (1984); this paper	45621.3–46348.5	467	V	HR 540	4 Per

instance, that some additional physical mechanism, acting in only some region of the log $T_{\rm eff}$ vs. log g plane, or a certain type of spin-orbit resonance is needed to excite the pulsations. (Note that the first attempt in this direction – though motivated differently – has been carried out by Harmanec et al. 1990 for the eclipsing binary RY Per and ended with a negative result.)

On the practical side, we intend to proceed in several steps: Since the detection of the orbital eccentricity is observationally more straightforward than the detection of non-synchronous rotation (which requires the knowledge of the stellar radius and inclination), we first compiled a tentative list of known bright northern-sky binaries with eccentric orbits and periods shorter than some 30 days, which have O, B or A-type primaries. Observations of these stars have begun with a Reticon 1872 detector installed at the coudé focus of the Ondřejov 2.0-m reflector. In the future, the promising candidates found in this preliminary search will be re-observed with a better time resolution using a blue-sensitive CCD detector. Moreover, a wider international collaboration is also being used. An inevitable step in this preparatory phase of the project is the determination of improved orbital elements for the binaries in question and their basic physical elements. It is clear that this step is vital for the success of the planned project.

This paper reports on the first results of the project: a detailed investigation of V436 Per, an eclipsing binary in an eccentric orbit without a published orbital solution and the first detection of its line-profile changes.

3. Current knowledge about V436 Per

V436 Per (1 Per, HR 533, HD 11241, BD+54°396, SAO 22690; V=5$^{\rm m}$.52, $B-V=-0^{\rm m}.18$) is an astrophysically interesting object. Although its variable RV was announced already by Adams (1912), the star was not observed very often and no clear picture of its character had emerged from spectroscopy. Blaauw & van Albada (1963) who analyzed their McDonald RVs, along with six Dominion Astrophysical Observatory (hereafter DAO) RVs published earlier, concluded that V436 Per is a spectroscopic binary with a period of 15$^{\rm d}$.6, $e=0.45$ and $K=10$ km s^{-1}. Beardsley (1969) published a collection of 59 Allegheny RVs of V436 Per from the years 1912–1915 and speculated about the presence of very rapid RV variations characteristic of the β Cep stars.

A better understanding of the system came from photometry. Kurtz (1977) used V436 Per as a comparison star in his Stromgren y observations of the Am star HR 540 and discovered that it is an eclipsing binary. However, he was unable to find the correct orbital period.

The eclipsing-binary nature of V436 Per was confirmed, and the orbital period was derived on the basis of a long series of visual observations carried out by the GEOS (an amateur group of European observers) since 1975 – see Figer & Maurin (1979). They derived a period of

$25^{\rm d}.93886 \pm 0^{\rm d}.00070$

and concluded from the position of the secondary minimum that the orbit is eccentric ($e \sim 0.6$). In an internal report, Figer (1980) argued that the orbital period had been decreasing steadily from 25$^{\rm d}$.939 in 1977 to 25$^{\rm d}$.933 in 1980.

The result of GEOS prompted North and Rufener to analyze Geneva V photometry of the star along with Kurtz's y data, derive a period of

$25^{\rm d}.9359 \pm 0^{\rm d}.0005$

and improve other elements to $e=0.30$ and $\omega = 116^\circ.7$ (see North et al. 1981). They estimated an inclination $i=87^\circ.9$ and suggested that the binary consists of two B2 stars. They also plotted available published RVs vs. phase of the orbital period but the RV curve did not look particularly convincing. Moreover, North et al. (1981) noted that its amplitude was much lower than that expected for their working model of the binary.

Further photoelectric observations of V436 Per were contributed by Percy (1982), Poretti (1982, 1984) and Böhme (1984). Recently, historical photoelectric observations of V436 Per by Güssow (1929) were transformed into the standard Johnson B magnitudes by Božić et al. (1995).

Gaspani (1982) presented a solution of the light curve published by North et al. (1981) and derived photometric radii

$r_g = 0.0381 \pm 0.0003$ and $r_s = 0.0331 \pm 0.0002$

for the greater and smaller star, respectively, (identifying the primary minimum as transit) as well as

$i = 88^\circ.3 \pm 0^\circ.9$, $e = 0.309 \pm 0.008$, $\omega = 115^\circ.9 \pm 0^\circ.7$,

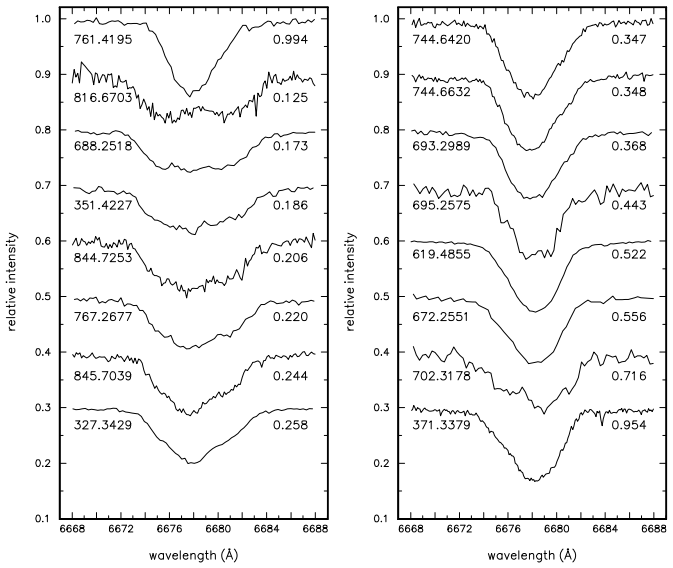

Fig. 1. The He I 6678 line profiles of V436 Per from some of the electronic spectra at our disposal. Equidistant offsets for 0.1 in relative intensity were chosen but the corresponding HJDs−2449000 and orbital phases from the primary mid-eclipse are given with each profile. The blending of the lines from two binary components creates an illusion of line-profile changes.

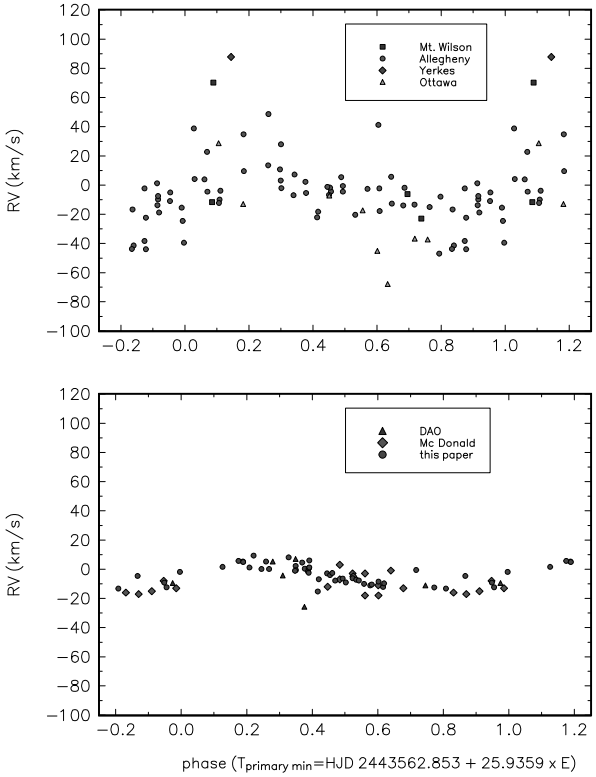

Fig. 2. A phase plot of historical **a** and more recent **b** RVs of V436 Per based on the ephemeris of North et al. (1981)

$$L_g = 0.73 \pm 0.03 \text{ and } L_s = 0.27 \pm 0.03 \ .$$

4. Observations and reductions

4.1. Spectroscopy

New electronic spectra of V436 Per were obtained at three observatories: at Ondřejov (2.0-m reflector, coudé, 17 Å/mm Reticon spectra, 6300–6700 Å), at the DAO (1.2-m coudé and 1.8-m Cassegrain, 10 Å/mm CCD 4096 spectra, 6100–6700 Å) and at the Haute Provence Observatory (1.52-m reflector, coudé, Aurélie spectrograph). Initial reductions of the DAO spectra and their conversion into 1-D images were carried out by SY using IRAF; all other reductions were carried out by PH with the help of the SPEFO software (developed by the late Dr. J. Horn). Each wavelength calibration was based on Th-Ar comparison spectra but the zero point of the wavelength scale was corrected individually through the measurements of selected atmospheric lines; for details, see Horn et al. (1996). Thanks to this last step, the reduced spectra from all three instruments are safely on the same heliocentric wavelength scale for all practical purposes.

We also compiled the published RVs based on photographic spectra. A journal of all RV data files is presented in Table 1.

The line spectrum of V436 Per is not very rich in the red spectral region. The only two strong lines are Hα and He I 6678. One can also note weak Si II 2 lines at 6347 and 6371 Å, Ne I 1 line at 6402 Å, and C II 2 lines at 6578 and 6583 Å, located in the red wing of the Hα line. A representative selection of the He I 6678 line profiles from electronic spectra is shown in Fig. 1. Obviously, most of the observed variations can be attributed to blending between the two binary components. However, only in a few cases could one distinguish the separate line cores of each star. To be able to compare our RVs with those published by other investigators on the basis of photographic spectra, we deliberately measured the RV, utilizing only the wings of Hα and He I 6678 lines. A plot of these RVs vs. phase of the known orbital period is shown in Fig 2, separately for the published and new data. A low-amplitude RV variation is clearly seen but it is obvious that it does not describe the orbital motion of the components of V436 Per properly. Obviously, the lines from both components are heavily blended at all orbital phases and the degree of this blending also depends on the dispersion and resolution of the spectrograms.

4.2. Photometry

We compiled the sets of yellow and blue observations of V436 Per. The journal of photoelectric observations at our disposal is presented in Table 2. The only new observations are several night series of V observations obtained by one of us, EP. They represent a direct continuation of his earlier observations – cf. Poretti (1984). The yellow and blue magnitude differences V436 Per − HR 540 were increased by $6\overset{\text{m}}{.}45$ and $6\overset{\text{m}}{.}63$, respectively (V and B magnitudes of HR 540); blue magnitude differences obtained by Güssow (1929) were converted to B magnitudes following Božić et al. (1995); the accurate B magnitudes of the comparison stars 4 Per and 2 Per derived by Harmanec et al. (1994) were used; the all-sky Geneva B observations were used in their original form (their zero point is about

Table 4. First solutions of the combined yellow and blue light curve

Element	solution 1 unweighted	solution 2 weighted
$P_{\rm sider.}$ (d)	25.935890	25.935871
$P_{\rm anom.}$ (d)	25.935980	25.936024
rms	0.000017	0.000014
dω/dt ($^\circ$ yr^{-1})	0.0177± 0.0053	0.0299± 0.0041
$T_{\rm periastr.}$	43563.356	43563.375
rms	0.017	0.015
$T_{\rm prim.ecl.}$	43562.858	43562.857
$T_{\rm sec.ecl.}$	43573.585	43573.591
e	0.4084± 0.0051	0.4015± 0.0044
ω ($^\circ$)	107.87± 0.30	108.19± 0.27
i ($^\circ$)	88.081± 0.025	88.082± 0.025
r_1	0.04188± 0.0010	0.04285± 0.0008
r_2	0.03757± 0.0012	0.03649± 0.0011
L_1 in V	0.543± 0.026	0.570± 0.024
L_1 in B	0.5 fixed	0.523 fixed
$y_{\rm Kurtz}$	5.4917± 0.0009	5.4898± 0.0007
rms	0.0062	0.0054
$V_{\rm Geneve}$	5.5165± 0.0009	5.5164± 0.0009
rms	0.0116	0.0118
$V_{\rm Por1}$	5.5128± 0.0012	5.5128± 0.0011
rms	0.0099	0.0098
$V_{\rm Por2}$	5.5197± 0.0008	5.5198± 0.0007
rms	0.0097	0.0097
$V_{\rm Bohm}$	5.5223± 0.0091	5.5225± 0.0092
rms	0.0398	0.0399
$B_{\rm Gus1}$	5.3507± 0.0029	5.3507± 0.0029
rms	0.0112	0.0112
$B_{\rm Gus2}$	5.3684± 0.0047	5.3684± 0.0047
rms	0.0106	0.0106
$B_{\rm Geneve}$	4.3368± 0.0010	4.3367± 0.0010
rms	0.0132	0.0133
$b_{\rm KPNO}$	5.5666± 0.0007	5.5667± 0.0007
rms	0.0034	0.0034
mean rms	0.0116	0.0090
No. of obs.	1078	1078

Notes: $P_{\rm sider.}$ and $P_{\rm anom.}$ denote the sidereal and anomalistic orbital period, respectively. The anomalistic period is defined as the time elapsed between two consecutive periastron passages; it is, therefore, usually used to the calculation of orbital phases. The quoted values of ω and dω/dt are given for the epoch of periastron passage of each solution. The "mean rms" is the mean rms error of one observation of unit weight for the solution; all errors quoted with individual elements are rms errors of these elements calculated from the cross-correlation matrix.

$1\overset{\rm m}{.}0$ brighter than the zero point of the Johnson B magnitudes). Since only 163 Geneva B observations are available, our complete set of yellow and blue data consists of 1078 individual observations. For the convenience of future investigators, we publish these data in detail in Table 3.[1]

[1] Table 3 is only available in electronic form: see the Editorial in A& AS 103, No.1 (1994)

5. Constant or varying orbital period?

A closer inspection of Fig. 2 and the photometric data reveals several facts relevant to this problem:

• More recent RV data sets, shown in the lower panel of Fig. 2, agree well with each other and define a RV curve with a full amplitude of about 15 km s^{-1}, maximum near phase $0\overset{\rm P}{.}25$ and minimum near phase $0\overset{\rm P}{.}87$.

• The early RV data define a RV curve with a larger amplitude and a great deal of scatter. At first sight, it seems that the maximum and minimum of this curve occur at earlier orbital phases than those for the more recent data. This, however, may be an apparent effect caused by those few observations in which – as we guess – the binary components were partly resolved close to the elongations of the binary. The bulk of the data still seems to define a RV curve similar to, and in phase with the more recent data.

• A tentative phase plot of all available photoelectric data for the period derived by North et al. (1981) showed that there is no reason to postulate a rapid period decrease suspected by Figer (1980).

To investigate the problem in a more quantitative way, we calculated formally several orbital solutions in which we kept the photometric value of the orbital eccentricity of 0.3 fixed. The orbital solutions were calculated with the computer program FOTEL developed by one of us (P. Hadrava) – see Hadrava (1990). (The latest version of the program and user guide can be obtained via anonymous ftp sunstel.asu.cas.cz (147.231.24.100), directory pub/fotel/.)

Not to get confused by too heterogeneous data at the beginning, we first calculated separate orbital solutions for the homogeneous set of Allegheny RVs and for a combination of McDonald RVs by Blaauw & van Albada (1963) and our new data. We obtained:

Old: P = $25\overset{\rm d}{.}837 \pm 0\overset{\rm d}{.}050$, $\omega = 246^\circ \pm 35^\circ$,
$T_{\rm max.RV}$ = HJD 2420018.0 ± 2.2
New: P = $25\overset{\rm d}{.}9352 \pm 0\overset{\rm d}{.}0022$, $\omega = 337^\circ \pm 21^\circ$,
$T_{\rm max.RV}$ = HJD 2443543.0 ± 1.5 .

Judging by the calculated errors, the old RVs seem to indicate a shorter orbital period while the more recent RVs agree very well with the ephemeris by North et al. (1981).

Using all available RVs, we then calculated another two orbital solutions, with and without the indicated period increase. It turned out that the solution for the secularly increasing period leads to an unrealistically high rate of the period increase of 171 s yr^{-1}. Moreover, the rms error of one observation for the solution with a variable period was *larger* than that for a constant period. This seems to indicate that the suspected period increase is spurious and that the available data are better reconciled on the assumption of a constant period.

The solution for the constant period for all (unweighted) RVs leads to

P = $25\overset{\rm d}{.}93535 \pm 0\overset{\rm P}{.}00087$,
$\omega = 294^\circ \pm 23^\circ$, $\gamma = -4.7 \pm 1.4$ km s^{-1},
$T_{\rm periastr.}$ = HJD 2443563.5 ± 1.6,
$T_{\rm max.RV}$ = HJD 2443566.2 .

This period agrees well with the period which follows from the solution for the more recent data only. It is also notable that the longitude of periastron passage obtained is about 180° higher than that from the solution of the light curve (Table 4; see below). This indicates that the RVs measured on line wings are more affected by the orbital motion of the binary component which is eclipsed during the secondary minimum.

Therefore – although neither a very slow apsidal motion nor a small secular change of the orbital period can be excluded completely – our analysis shows that the assumption of a constant orbital period represents a good approximation from a detailed analysis of available RV data on V436 Per.

6. Solution of the light curve

To obtain a new solution of the light curve of V436 Per, we again used program FOTEL and all yellow and blue observations available to us. Convenient features of FOTEL are that it allows calculation of individual zero points for individual data sets and also a simultaneous solution for observations in several different bandpasses. It is necessary to warn, however, that all available blue observations, with the exception of a single Geneva observation, were obtained *outside* the eclipses and do not allow determination of relative luminosities of both stars in the blue.

We proceeded in two steps. First, we calculated a solution in which all data were treated with equal weight. Then, we assigned each data set a weight inversely proportional to the square of the rms error of that data set calculated by FOTEL in the first solution and repeated the solution. We fixed the limb-darkening coefficients at a value of 0.3 in V and 0.4 in B for both stars. Trial calculations and investigation of residuals led us to suspect the presence of a very slow apsidal motion. Indeed, test calculations for several V data subsets indicated a small systematic increase in the value of the longitude of periastron with time. We therefore calculated the final two solutions with periastron advance as one of the elements. These solutions for unweighted and weighted data are given as solutions 1 and 2, respectively, in Table 4. It is seen that a very slow apsidal motion, significant with respect to its calculated error, was indeed found. Thanks to the very steep wings of the eclipses and their short duration with respect to the orbital period, the value of the orbital period is well constrained by the solution. The light curve, based on all observations and with the zero-points properly adjusted, is shown (separately for yellow and blue observations) in Fig. 3.

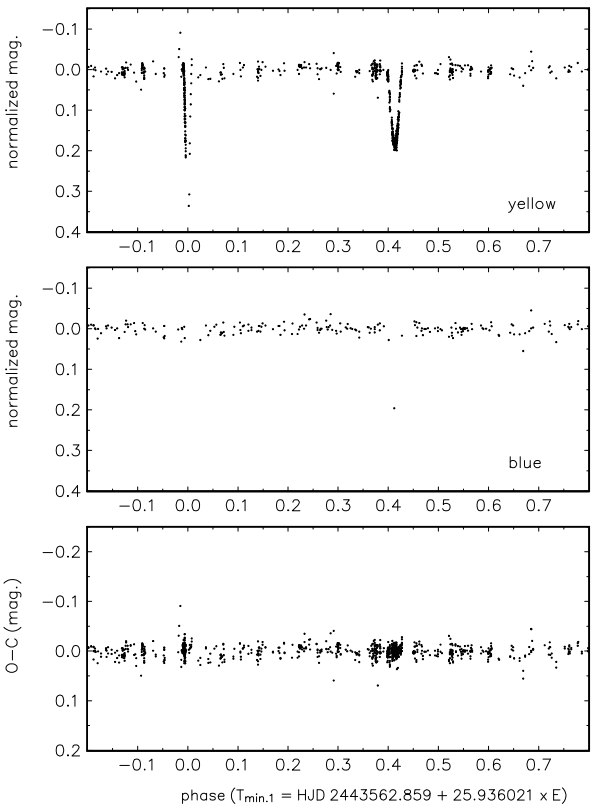

Fig. 3. The combined (and for each data set properly shifted) light curve of V436 Per, based on all observations in yellow and blue passbands, and the O−C deviations from the theoretical curve based on solution 2 of Table 4

7. Spectrum analysis and the orbital solution

7.1. Spectrum disentangling

A new efficient method of spectrum disentangling was recently proposed by Hadrava (1995). The computer implementation of this technique, Fortran program KOREL (a detailed description of the program can be obtained via anonymous ftp sunstel.asu.cas.cz (147.231.24.100), directory pub/fotel/), uses the parts of the observed spectra in the neighbourhood of selected spectral lines and solves for orbital elements of multiple systems with heavily blended line profiles. Relative weights can be assigned to individual spectra used in the orbital solution. The technique also allows inclusion of telluric lines and modelling of their temporal intensity changes. Besides the correct orbital elements, the original line profiles of the component stars can also be obtained and further investigated for their radiative properties and v sin i. Individual RVs of each star (and of telluric lines, too) are derived in KOREL via cross-correlation of the observed spectra with the decomposed line profiles of the star in question.

The electronic spectra cover a relatively short period of 813 d in comparison to nearly 3000 d covered by recent photoelectric photometry, or to nearly 22000 d if also historical photometry is included. Since our analysis indicated constancy of the orbital period, we adopted the period from the photometric solution 2 of Table 4, $25\overset{\mathrm{d}}{.}9360$, and kept it fixed in all solutions based on spectral disentangling.

Two different spectral regions (each one with 512 bins) were analyzed separately to check on the internal error of the method. This was necessary due to the fact that the current version of KOREL does not allow any objective calculation of errors of individual elements.

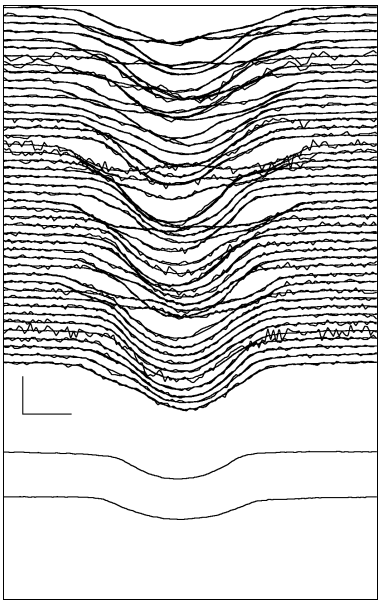

Fig. 4. The decomposition of He I 6678 . The line profiles of both component stars decomposed by KOREL are plotted at the bottom of the figure. The first 45 curves from the top represent the input spectra (in the same order as in Table 5), over which the profiles reconstructed from the decomposed profiles (with both RV's calculated from orbital elements and as independent free parameters for each exposure) are superimposed. The vertical and horizontal bar denote 10 per cent of the continuum level and 100 km s^{-1}, respectively

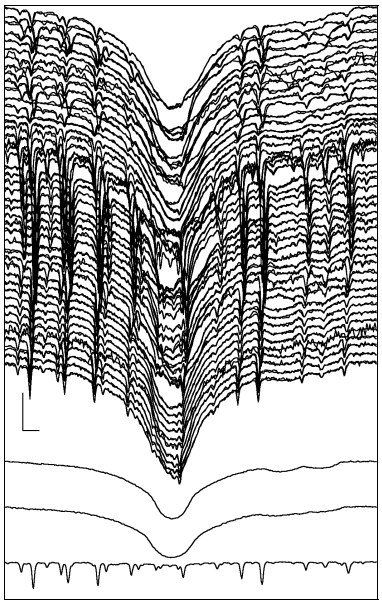

Fig. 5. The decomposition of Hα. The curve at the very bottom is the mean spectrum of telluric lines. The vertical and horizontal bar denote 10 per cent of the continuum level and 100 km s^{-1}, respectively

The first region ($\sim$6670–6687Å; see Fig. 4) contains the line of He I 6678 and was sampled with a step of 1.5 km s^{-1} per bin. Note that the spectral lines from individual binary components can only barely be resolved at the maximum RV separation (see, e.g., the profile JD ...816, the second one in Fig. 1). This region has been decomposed via KOREL as a two-component spectrum and the solution provided individual line profiles of both stars (cf. the bottom part of Fig. 4), RVs of both components for each spectrogram (given in Table 5) and a set of orbital elements – see Table 6. It is interesting to note that the only individual radial velocities measured by KOREL which deviate in the unweighted solution from the theoretical RV curve for more than 10 km s^{-1} correspond to spectra taken at JDs 2449927 and ...979, i.e. during the secondary minima of the binary. This is not surprising since during the eclipses the basic assumption of the spectrum decomposition, i.e. the constancy of line profiles, is not satisfied. It is encouraging, however, to see how sensitive the new method of disentangling is. In final solutions, the two spectra taken during the eclipse were given weights equal 0.01 (all other having unit weights).

In the second region ($\sim$6540–6590Å; see Fig. 5), both components of the Hα (scanned with a step of 4.5 km s^{-1} per bin) are heavily blended both with each other and the telluric lines. The spectrum in this region was, therefore, treated as resulting from *three* contributions. Besides individual line profiles of each binary component, their RVs for each spectrum and the orbital elements, also the relative intensities of the telluric spectra and their radial velocities (varying as the Earth moves around the Sun since the spectra are on a heliocentric wavelength scale) were obtained with KOREL. The good performance of the program can be judged from the fact that the ecliptic latitude and longitude of V436 Per were both obtained with errors of about 1° only. It is of interest to note that the disentangled Hα profiles of the components became smoother when the spectrum with the strongest telluric lines had been included. This way, the presence of the telluric lines – which usually complicates the analysis of the spectrograms in the red and IR spectral regions – may turn into an advantage for the purpose of disentangling.

The method of line photometry (see Hadrava 1996) confirms the decrease of intensity of the secondary lines for the two exposures taken during secondary eclipse. Using it, we were able to find that the ratio of continua of the two stars is close to 1 (we get $I_1/(I_1 + I_2) = 0.501$ and 0.508 for the continua in the neighbourhood of He I 6678 and Hα, respectively). This is consistent with the photometric solution.

It is obvious from Table 6 that the solutions for both regions are in good agreement. However, it must be noted that while the solution for He I 6678 smoothly converged to the same set of resulting orbital elements in a wide range of initial approximations, the solution for Hα found several local shallower minima unless it was started close to the former solution. The small differences between solutions found directly by KOREL and the fit by FOTEL to RV's calculated by KOREL can be understood as a consequence of different weights of individual exposures in both methods. The orbital RV curves of both binary components, based on mean Hα and He I 6678 KOREL RVs from Table 5, are shown in Fig. 7.

Table 5. Radial velocities of V436 Per by KOREL and cross-correlation with orbital phases calculated from the primary mid-eclipse

HJD	phase	He I 6678		Hα			cross-correlation	
-2400000		RV_1	RV_2	RV_1	RV_2	$RV_{tell.}$	RV_1	RV_2
Reticon								
49327.3429	.258	−69.20	72.27	−67.53	73.35	−9.91	−74	69
49351.4227	.186	−92.99	95.93	−94.74	100.42	−17.82	−72	120
49619.4855	.522	23.14	−22.13	17.84	−12.37	18.41	8	8
49672.2551	.556	32.60	−33.88	27.46	−31.64	−0.61	54	−39
49688.2518	.173	−99.29	98.95	−98.16	106.03	−8.53	−86	111
49693.2989	.368	−27.57	29.13	−28.33	31.35	−9.00	−47	34
49695.2575	.443	7.88	3.30	−9.05	6.16	−8.67	−3	−3
49702.3178	.716	73.68	−73.33	66.36	−71.59	−13.21	83	−72
49761.4195	.994	−20.90	14.71	−19.33	−0.66	−24.03	6	6
49767.2677	.220	−79.94	85.53	−81.25	87.78	−22.13	−62	104
50017.4404	.866	85.63	−85.15	85.62	−89.34	4.21	74	−100
50081.2656	.326	−43.68	44.76	−41.61	44.62	−23.06	−34	72
50097.3604	.947	50.87	−53.89	49.99	−52.61	−22.21	55	−71
50114.3047	.600	40.04	−42.41	43.75	−43.98	−23.55	36	−80
Aurélie								
49371.3379	.954	38.45	−41.85	39.32	−45.98	−23.39	48	−53
DAO								
49744.6420	.347	−36.15	37.69	−36.30	37.98	−21.79	−56	29
49744.6632	.348	−37.12	37.19	−35.74	34.36	−22.24	−55	32
49816.6703	.125	−108.13	113.89	−106.50	114.52	−9.60	−109	120
49844.7253	.206	−88.74	91.17	−90.91	94.09	−1.33	−84	98
49845.7039	.244	−73.13	74.57	−70.29	75.77	−0.33	−73	76
49927.9616	.416	−14.95	14.32	−17.25	17.13	21.64	−31	36
49928.9203	.453	−1.64	2.83	−0.46	4.15	23.28	−8	−8
49929.9467	.492	10.57	−9.94	9.81	−7.63	22.75	−5	−5
49930.9880	.532	22.68	−25.29	21.33	−22.62	21.43	33	−27
49947.9756	.187	−94.59	96.18	−94.73	94.23	22.38	−88	102
49950.0235	.266	−65.46	67.25	−62.77	67.72	22.33	−63	72
49978.0157	.345	−34.11	36.44	−35.48	34.83	18.27	−57	27
49978.8098	.376	−25.72	25.86	−23.34	26.10	18.05	−39	30
49979.9180	.419	−14.95	21.46	−12.89	26.09	18.73	−48	6
49980.9779	.460	1.39	3.38	0.01	0.65	17.61	−4	−4
49983.9786	.575	33.22	−35.88	32.01	−35.95	17.21	38	−50
49984.9971	.615	41.74	−45.53	39.63	−44.04	17.39	55	−46
50033.0856	.469	6.24	−7.75	5.96	−5.17	−0.46	−7	−7
50040.9156	.771	76.29	−77.52	77.77	−81.04	−4.89	71	−86
50041.8440	.806	82.48	−85.33	80.96	−84.51	−3.91	74	−97
50056.8651	.386	−20.53	22.06	−21.50	22.95	−9.45	−43	34
50056.9055	.387	−19.67	20.30	−22.95	21.64	−8.15	−56	15
50056.9248	.388	−19.05	21.36	−22.74	21.78	−9.89	−54	16
50056.9422	.389	−19.16	20.76	−22.80	23.87	−8.64	−63	11
50056.9596	.389	−22.29	22.23	−23.27	21.32	−10.52	−49	25
50056.9692	.390	−18.97	22.15	−22.30	23.89	−8.52	−29	43
50137.6661	.501	11.68	−13.57	13.66	−13.37	−22.57	15	−7
50138.6880	.540	19.99	−18.41	22.46	−28.08	−21.55	41	−11
50139.6982	.579	34.58	−36.53	31.60	−36.26	−21.69	56	−38
50140.6808	.617	43.73	−46.65	43.12	−46.56	−21.25	53	−53

Table 6. Orbital elements derived with KOREL and by the standard cross-correlation technique

element	photometry	KOREL He I 6678	KOREL Hα	KOREL+FOTEL mean He & Hα	cross-cor.+FOTEL He I 6678
$P_{\rm anom.}$ (d)	25.936024± 0.000014	fixed	fixed	fixed	fixed
T_0 (HJD−2400000)	43563.375± 0.015	43563.529	43563.563	43563.238±.050	43563.22±.34
e	0.4015±0.0044	0.380	0.395	0.3755±.0057	0.336±.031
ω (deg.)	108.19±.27	109.7	109.6	105.7±0.74	102.0±4.7
K_1 (km s^{-1})	–	95.9	96.7	97.3±1.0	95.3±5.5
K_2 (km s^{-1})	–	101.3	104.4	101.6±1.0	107.6±6.6
rms (km s^{-1} or mag.)	0.0090	–	–	2.48	13.4

7.2. Cross-correlation radial velocity measurements

To have an independent check on the new technique of spectrum disentangling described above, we also measured the RVs from the spectra of V436 Per using a digital cross-correlation technique. Additional background on the topic of cross-correlation radial velocity measurement may be found in the paper by Simkin (1974). One of us (DH) has developed a computer program for cross-correlating stellar spectra, similar to the VCROSS program developed by Hill (1993). This computer program also allows for the fitting of blended cross-correlation function (ccf hereafter) peaks using either analytic (Gaussian or Lorentzian) or digital line profile functions. The latter technique is discussed, for example, by Hill and Holmgren (1995). The program, CCF3, runs interactively on a 486 PC, complete with graphical output.

The comparison star chosen for the cross-correlation measurements was ζ Cas (HR153), since its spectral type (B2IV) is very similar to those of the components of V436 Per. Moreover, ζ Cas is a slow rotator, with $v \sin i = 18$ km s^{-1}. The mean RV of ζ Cas was measured to be -2.8 ± 0.4 km s^{-1}, using the interactive spectral reduction program SPEFO. It rests on the measurements of the following lines: Ne I 6334, Si II 6347, Si II 6371, N II 6379, Ne I 6382, Ne I 6402, H I 6562, C II 6578, N II 6610, He I 6678, and O II 6721.

As with other spectra from Ondřejov, telluric line radial velocities were used to put the ccf RVs on the same system as all other RVs.

Like in the spectrum disentangling by KOREL, all spectra used in the cross-correlation measurements were first converted to a logarithmic wavelength scale, and then re-interpolated using a constant step size in ln λ. This is necessary because a radial velocity shift is equivalent to a constant shift in ln λ.

The cross-correlation measurements of V436 Per were limited to the He I 6678 line, since only it and Hα are visible on most of our spectra. Hα was not used since its inclusion would result in a very broad ccf peak. Moreover, this line has numerous telluric absorption lines superimposed on it. A typical ccf close to the maximum RV separation is shown in Fig. 6. To measure RVs from the severely blended ccf peaks of V436 Per, we resorted to fitting digital profiles to the ccf peaks, and fixing the width of the secondary's ccf peak to ensure some consistency between the measurements. The digital profile was constructed from a ccf (spectrum 6047) close to conjunction, and the secondary's width was estimated from reliable preliminary fits of ccfs close to the maximum radial velocity separation. The resulting radial velocity curve is also shown in Fig. 7. Note that V436 Per represents a severe test for the cross-correlation method since the line widths of the components are comparable to the maximum RV separation. At no orbital phase are the ccf peaks completely resolved.

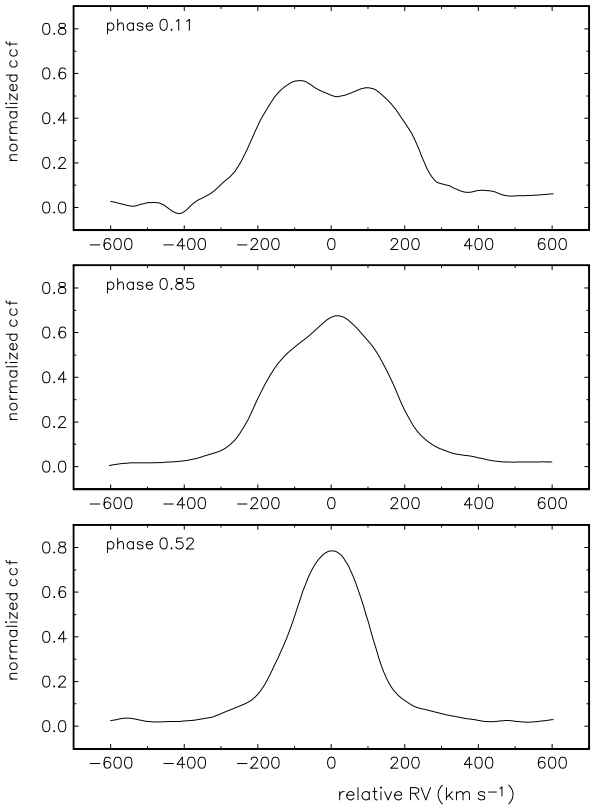

Fig. 6. Examples of ccfs from several orbital phases

It is, of course, of great interest to compare the RVs from the cross-correlation and disentangling techniques. The radial

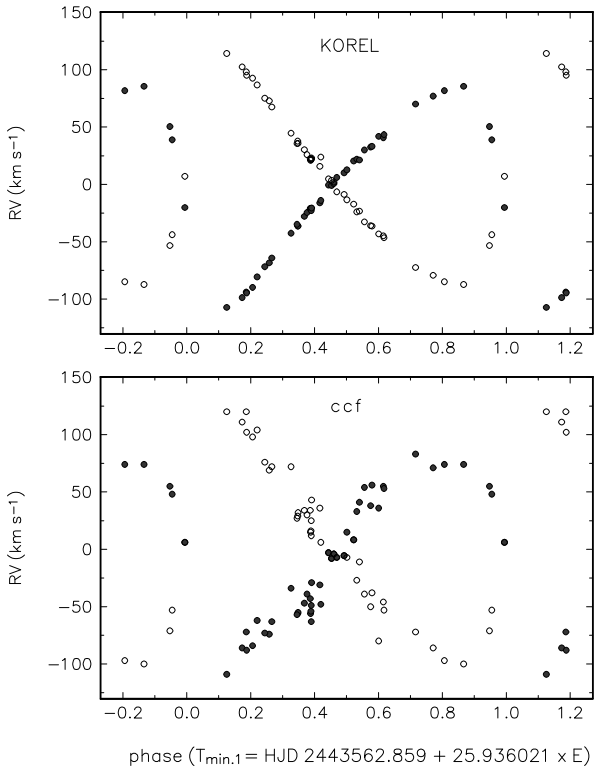

Fig. 7. A comparison of the RV curves of both binary components derived by KOREL and by cross-correlation technique. Primary and secondary are denoted by black and open circles, respectively. Superiority of KOREL is clearly seen

velocities obtained by both methods are presented in Table 5 and the corresponding orbital elements in Table 6. To this, we add the systemic velocity of -1.6 ± 1.5 km s^{-1}, which could only be derived for ccf RVs (calibrated in their zero point as discussed above). Fig. 7 illustrates the differences between the two data sets. In general, the RVs derived by both methods are comparable, but those from the cross-correlation method show a greater scatter and result in somewhat different semi-amplitudes of the RV curves. Consequently, we have adopted the data set from KOREL as the final one.

In passing we note how instructive it is to compare the RV curves derived here to the RV curve based on the standard measuring technique (cf. Fig. 2) which fails completely for binaries similar to V436 Per.

8. Basic physical elements of the binary

8.1. Masses, radii and radiative properties

To obtain the final values of the masses, radii and other basic physical elements of the binary, we adopted the mean (Hα and He I 6678) RVs from KOREL and used FOTEL to calculate the final set of elements based on *simultaneous* solution of the light and RV curves. In doing so, we adopted the result from the spectral disentangling (line photometry) and assumed $L_1 = L_2$ in the solution. The reason why we believe that the spectroscopic result is currently more reliable than the photometric one is that the available photometry *does not cover* the very bottom of the primary minimum. Relative weights of photometry and spectroscopy were chosen in such a way as to allow both data sets to affect the solution with comparable strengths (i.e. that each is responsible for about one half of the sum of squares of O-C). The main results of this combined solution are summarized in Table 7.

Table 7. Final set of the orbital and photometric elements derived from the combined solution with FOTEL

$P_{\rm anom.}$ (d)	25.936021± 0.000015
$P_{\rm sider.}$ (d)	25.935872
$T_{\rm periast.}$ (HJD−2400000)	43563.420± 0.016
$T_{\rm prim.min.}$ (HJD−2400000)	43562.859
$T_{\rm sec.min.}$ (HJD−2400000)	43573.591
dω/dt (deg. yr^{-1})	0.0292± 0.0043
e	0.3882±0.0043
ω (deg.)	108.98±0.27
K_1 (km s^{-1})	98.0± 1.0
K_2 (km s^{-1})	102.5± 1.2
$M_1 \sin^3 i$ (M$_\odot$)	8.67
$M_2 \sin^3 i$ (M$_\odot$)	8.30
$A \sin i$ (R$_\odot$)	94.75
i (deg.)	88.044± 0.020
r_1	0.04041± 0.00055
r_2	0.03923± 0.00042
L_1/L_2	1.0 fixed
rms (km s^{-1})	2.90
rms (mag.)	0.0091

As we have already remarked, only yellow photometric observations cover both binary minima. It is, therefore, impossible to estimate individual colour indices of the binary components from photometry. One can only use the mean calibrated photometry of the binary outside of eclipses to estimate the average radiative properties of the binary components (taking into account their obvious similarity).

Perhaps the most accurate of such estimates that can be obtained is from the mean Geneva colours using a recent calibration by Künzli et al. (1996). One obtains $T_{\rm eff.}$ = (21750 ± 340) K and log g = 4.18 ± 0.22 [CGS]. (The quoted errors are the formal errors of the new calibration.)

As a check, we also used Johnson and Strömgren values for the whole binary published by Crawford (1963):

$V = 5\overset{\rm m}{.}52$, $B - V = -0\overset{\rm m}{.}188$, $U - B = -0\overset{\rm m}{.}837$;

and by Crawford et al. (1971):

$V = 5\overset{\rm m}{.}50$, $B - V = -0\overset{\rm m}{.}17$, $U - B = -0\overset{\rm m}{.}82$;

$b - y = -0\overset{\rm m}{.}080$, $m_1 = 0\overset{\rm m}{.}088$, $c_1 = 0\overset{\rm m}{.}104$, $\beta = 2\overset{\rm m}{.}650$

and two recent calibrations (see Napiwotzki et al. 1993, Balona 1994). This lead to $T_{\rm eff.}$ = 21300 – 22600 K, log g = 4.4 and R = 4.3 R$_\odot$. The range of the effective temperatures corresponds well to a spectral class B2.

Table 8. Basic physical elements of V436 Per

Element	primary	secondary
$M/M_\odot$	8.69	8.31
$R/R_\odot$	3.83	3.72
log g [CGS]	4.21	4.22
$T_{\rm eff.}$ (K)	21750	21750
$M_{\rm bol}$	−4.09	−4.03
M_V	−1.89	−1.83
$v_{\rm obs.}$ sin i (km s^{-1})	120	135
$v_{\rm syn.}$ sin i (km s^{-1})	18.4	17.9

Basic physical elements of V436 Per are summarized in Table 8. They are based on the results of the combined solution presented in Table 7 and on the *mean* $T_{\rm eff.}$ derived from the photometric calibration. We have not attempted to assign errors to values in Table 8. The present version of KOREL is unable to produce realistic errors of the orbital elements on account of the complexity of the problem and also the true errors of log g and $T_{\rm eff.}$ are hard to estimate. We, therefore, feel that it would not be fair to quote errors which would be purely formal. Comparing the values of masses and radii of Table 8 with Harmanec's (1988) compilation of accurate masses and radii one finds that we arrived at values which correspond reasonably well to normal stars of spectral class B2. It is also encouraging to see a very good agreement between the values of log g derived from masses and radii and from radiative properties of the stars. All this certainly increases the credibility of the result. It is clear, however, that our values are not definitive. More observational effort will be needed to cover the centre of the primary minimum with photometric data, to obtain calibrated photometry in some well-defined system and to secure more spectra at certain still little-covered orbital phases.

It is clear, however, that the new technique of the spectrum disentangling is a very powerful tool for the analyses of heavily blended binary spectra. Though preliminary, our basic physical elements collected in Table 8 certainly represent the first realistic determination of masses and radii of the binary components of V436 Per. Note that these results could never have been obtained with the classical method of RV measurement, and would be much less accurate with the cross-correlation technique.

8.2. Rotational velocities

Using the line profiles of individual binary components, reconstructed by KOREL, we also derived the v sin i values for both stars. The observed (disentangled) and calculated theoretical LTE line profiles are compared in Fig. 8.

Synthetic spectra for our analysis were calculated from the Kurucz (1993b) grid of solar composition LTE line blanketed model atmospheres with the help of a computer code SYNSPEC (for a description see Hubeny et al. 1994). Oscillator strengths, wavelengths and damping parameters for all lines contributing to the resulting spectrum in the neighbourhood of the line profiles in question were taken from the list of Kurucz (1993a). The Stark broadening of hydrogen Balmer lines was calculated using the tables of Vidal et al. (1973), and the Stark profile of the He I 6678 line was calculated after Dimitrijević & Sahal-Bréchot (1984). The synthetic spectra resulting from SYNSPEC were rotationally broadened with help of the computer code SPEFO.

After trial comparisons of synthetic spectra for different rotational velocities with the observed ones it turned out that the best fit to the Hα region can be obtained for $T_{\rm eff.}$ = 22000 K (a Kurucz model with $T_{\rm eff.}$ closest to our estimate of 21750 K), log g = 4.0, and v sin i = 120 km s^{-1} for the primary, and for v sin i = 135 km s^{-1} and the same effective temperature and gravity as before for the secondary.

Considering all uncertainties involved, we think that the agreement of the observed and calculated profiles is very satisfactory for the Hα line and C II lines. Note in particular how well the small extra absorption between both C II lines for the secondary is matched by the synthetic spectrum. We stress that this feature is a result of line blending, not a separate line, and occurs for only a narrow interval of rotational velocities. The agreement is less satisfactory for the He I 6678 line. However, this line is known to be prone to NLTE effects and is often observed stronger for the B stars than the LTE theory predicts (Auer & Mihalas 1973, Dimitrov & Kubát 1988). NLTE effects can also partly affect the core of the Hα line and the C II line intensities. Nevertheless, since we do not aim at an exact determination of effective temperature and gravity by means of synthetic spectra, the above differences are not substantial. Our goal was the determination of rotational velocities and both fits appear good for this purpose. This is also true for the other two very weak spectral lines, Si II and Ne I, which were also decomposed with KOREL.

In Table 8 we compare the observed v sin i values with the values expected for the spin-orbit synchronization at periastron (cf. Harmanec 1988). It is seen that both components of V436 Per rotate much faster than expected for the synchronization. The corresponding rotational periods are $1\overset{\rm d}{.}6$ and $1\overset{\rm d}{.}4$ for the primary and secondary, respectively.

8.3. Apsidal motion

The theoretical apsidal motion rate for V436 Per was calculated using the tables of internal structure constants calculated by Claret and Giménez (1992). Specifically, we have used their Table 17 and assumed abundances of X = 0.70 and Z = 0.02. To calculate the apsidal motion rate, the usual equations have been used (eg., Claret and Giménez, 1993) including the relativistic apsidal motion rate (eg., Giménez, 1985). The total apsidal motion rate is 7.692×10^{-3} degrees per year, which corresponds to an apsidal period of 46800 years. It is interesting to note that the relativistic rate is larger than the classical one: $\omega_{rel} = 6.819 \times 10^{-3}$ degrees per year, while $\omega_{cl} = 8.731 \times 10^{-4}$ degrees per year.

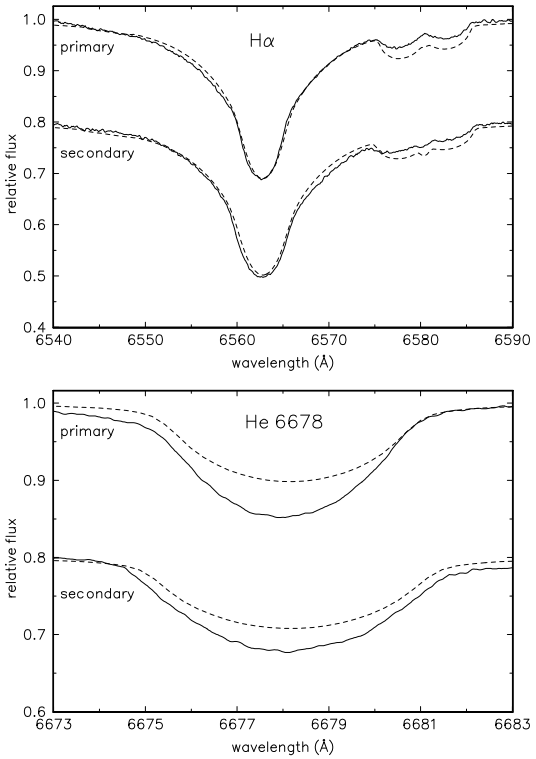

Fig. 8. A comparison of the observed (disentangled) and calculated LTE line profiles of both binary components. Projected rotational velocities of theoretical line profiles are 120 and 135 km s^{-1} for the primary and secondary, respectively. Theoretical line profiles are shown by dashed lines and the profiles for the secondary are shifted for 0.2 in relative intensity

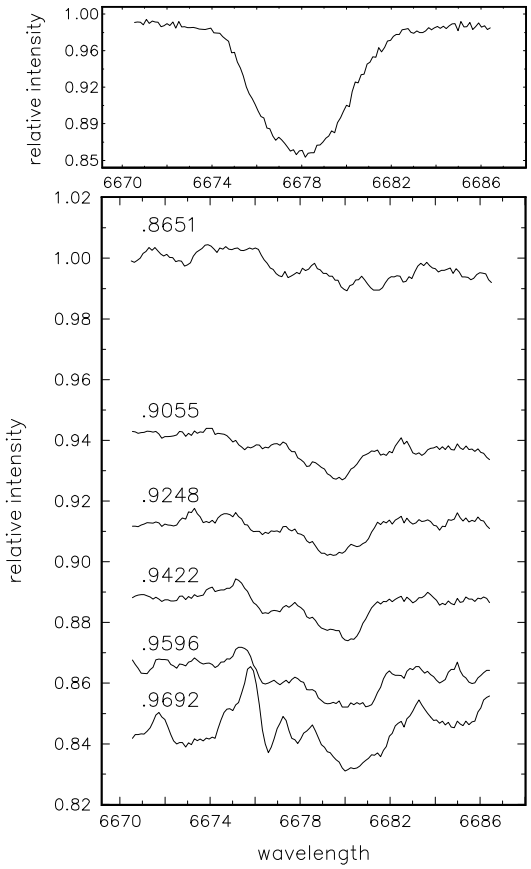

Fig. 9. Difference spectra in the neighbourhood of the He I 6678 line from the Dec.1, 1995 series of the DAO spectra. Disentangled profile from KOREL was subtracted from the individual observed profiles. Sub-features of apparent absorption, moving from the blue to red across the line profiles, are clearly seen. The offset of the spectra is proportional to the times of mid-exposures which are given for each exposure in HJD−2450056. The S/N ratio of the spectra is between 330 and 400, with the exception of the last one which has only 120. The line profiles were filtered with a 0.6 Å wide filter. The upper panel shows one DAO line profile of He I 6678 (phase $0^{p}.389$) to indicate the wavelength range over which the line extends.

Our – certainly uncertain – observational result implies an apsidal period of 12 300± 1900 yrs and clearly needs verification by future observations.

9. Discovery of rapid line-profile changes

The excellent practical performance of the new method of disentangling, even in such complicated cases as V436 Per, opens the way to a much more objective search for rapid line-profile changes. While the usual practice has been to create the difference spectra with respect to the mean spectrum of the night (or longer) series of spectrograms, one now can subtract the sum of the decomposed individual profiles, properly shifted in RV for the given phase of the known RV orbit, from the individual spectra of the series. A critic of this procedure may object that if line-profile variability is present, the basic principle of the disentangling method of Hadrava (1995) that the profiles are constant is violated. We believe, however, that this need not be so in practice. First, the amplitude of line-profile variations is always small in comparison to the strength of the profiles themselves and second, the line-profile variations occur on timescales much shorter than the orbital period. This means, in practice, that if one obtains rich enough series of spectrograms, well distributed in orbital phase, the line-profile variations represent something like high-frequency noise to the basic binary line profiles. Therefore, the original, undisturbed line profiles should still be recovered by KOREL. In future, we shall carefully test this conjecture on the spectra of binaries with well resolved line profiles of individual binary components.

The observational material, currently available to us, is not very suitable to a search for rapid line-profile changes. The only night series consists of 6 DAO spectra taken over a period of $0^{d}.11$. The first five spectra have S/N between 330 and 400 but the last one has a S/N of only 120. To check on the presence of line-profile variations, we subtracted the synthesized KOREL profiles from the individual observed profiles. The corresponding difference spectra are shown in Fig. 9. The presence of moving subfeatures in the He I 6678 line is clearly seen. We measured RV of the strongest sub-feature, seen in the whole series, to derive an estimate of the acceleration with which it moves across

the line profile. The acceleration is $a_0 = 700$–1100 km s^{-1}, depending on whether or not the sub-feature in the first profile is the same feature as the strongest one seen in the other profiles or not. The lower value could roughly be reconciled with the rotational period of about $1\overset{d}{.}5$. At present, we are unable to identify which of the binary components is the line-profile variable since the Dec. 1 series was obtained close to a conjunction of the binary. If the detected variations are indeed due to forced oscillations, they could be expected for both binary components, given the mutual similarity of both stars found here.

10. Conclusions

A novel analysis of electronic spectra from three observatories and of all available photoelectric observations of V436 Per allowed us to derive the first reliable and internally consistent basic physical elements of this binary. This represents a practical proof of the extreme usefulness of the new method of spectrum disentangling devised by Hadrava (1995).

V436 Per is an astrophysically interesting system with highly eccentric orbit and a highly non-synchronous rotation of both binary components. The presence of a formally significant slow apsidal motion was detected but needs further verification in the future.

The present study is a part of a project aimed at identification of physical conditions under which forced oscillations are excited in close binaries with OBA components. Line-profile variations in the form of travelling sub-features were indeed detected in a series of spectra of V436 Per.

Acknowledgements. Some of the Ondřejov spectrograms used in this study were kindly obtained for us by Drs. J. Horn, K. Juza, V. Šimon and P. Škoda. The use of the computerized bibliography from the Strasbourg Astronomical Data Centre is also gratefully acknowledged. This study was supported by the grant 205/96/0162 of the Grant Agency of the Czech Republic and also by the project K1-003-601/4 *Astrophysics of non-stationary stars* of the Academy of Sciences of the Czech Republic. The Geneva photometric measurements were supported by the Swiss National Science Foundation. Finally, we gratefully acknowledge a very careful proofreading of the text and a number of useful suggestions by an anonymous referee which helped us to improve the presentation.

References

Aerts C., Mathias P., Gillet D., Waelkens C. 1994, A&A 286, 109
Abt H.A. 1970, ApJS 19, 387
Adams W.S. 1912, ApJ 35, 172
Auer L.H., Mihalas D. 1973, ApJS 25, 433
Baade D. 1983, Hvar Obs. Bull.7, 185
Baade D. (Ed.) 1991, *Rapid Variability of OB-Stars: Nature and Diagnostic Value*, ESO Conf. Proc. No. 36, ESO, Garching
Balona L.A. 1994, MNRAS 268, 119
Balona L.A., Henrichs H.F., Le Contel J.M. (Eds.) 1994, *Pulsation, Rotation and Mass Loss in Early-Type Stars*, IAU Symp. 162, Kluwer, Dordrecht
Beardsley W.R. 1969, Publ. Allegheny Obs. 8, No. 7
Blaauw A., van Albada T.S. 1963, ApJ 137, 791
Böhme D. 1984, Inf.Bull.Var.Stars No.2507
Božić H., Harmanec P., Horn J., Koubský P., Scholz G., McDavid D., Hubert A.-M., Hubert H. 1995, A&A 304, 235
Cannon J.B. 1918, Publ.Dominion Obs. Ottawa 4, 253
Chapellier E., Le Contel J.M., Le Contel D., Sareyan J.P., Valtier J.C. 1995, A&A 304, 406
Claret A., Giménez A. 1992, A&AS 96, 255
Claret A., Giménez A. 1993, A&A 277, 487
Crawford D.L. 1963, ApJ 137, 523
Crawford D.L., Barnes J.V., Golson J.C. 1971, AJ 76, 1058
Dimitrijević M.S., Sahal-Bréchot S. 1984, JQSRT 31, 301
Dimitrov D.L., Kubát J. 1988, Bull. Astron.Inst.Czechosl. 39, 265
Figer A., Maurin L. 1979, GEOS Circular on Eclipsing Binaries EB2, Paris, January 12, 1979
Figer A. 1980, Note Circulaire GEOS NC 253, Paris, Oct. 2, 1980
Fitch W.S. 1967, ApJ 148, 481
Fitch W.S. 1969, ApJ 158, 269
Frost E.B., Barrett S.B., Struve O. 1926, ApJ 64, 1
Gaspani A. 1982, Inf.Bull.Var.Stars No.2077
Giménez A. 1985, ApJ 297, 405
Güssow M. 1929, Astron. Nachr. 237, 321
Hadrava P. 1990, Contr. Astron. Obs. Skalnaté Pleso, 20, 23
Hadrava P. 1995, A&AS 114, 1
Hadrava P. 1996, A&A (submitted)
Harmanec P. 1988, Bull. Astron.Inst.Czechosl. 39, 329
Harmanec P. 1989, Bull. Astron.Inst.Czechosl. 40, 201
Harmanec P., Tarasov A.E. 1990, Bull. Astron.Inst.Czechosl. 41, 273
Harmanec P., Walker G.A.H., Matthews J.M. 1990, Be Star Newsletter No. 22, 12
Harmanec P., Horn J., Juza K. 1994, A&AS 104, 121
Hill, G. 1993, *New Frontiers in Binary Star Research*, eds. K.-C. Leung and I.-S. Nha, ASP Conference Series, 38, 127.
Hill, G., Holmgren, D.E. 1995, A&A 297, 127.
Horn J., Kubát J., Harmanec P., Koubský P., Hadrava P., Šimon V., Štefl S., Škoda P. 1996, A&A 309, 521
Hubeny I., Lanz T., Jeffery C.S. 1994, in Newsletter on Analysis of Astronomical Spectra No.20, C.S.Jeffery ed., St. Andrews University, p.30
Jaschek M., Groth H.-G. (Eds.) 1982, *Be Stars*, IAU Symp. 98, D. Reidel, Dordrecht
Kato S. 1974, PASJ 26, 341
Künzli, M., North, P., Kurucz, R.L., Nicolet, B., 1996, A&A (submitted)
Kurtz D.W. 1977, PASP 89, 939
Kurucz R.L. 1993a, Atomic Data for Opacity Calculations, Kurucz CD-ROM No.1
Kurucz R.L. 1993b, Solar Abundance Model Atmospheres, Kurucz CD-ROM No.19
Lee U. 1993, ApJ 417, 697
Lesh J.R., Aizenman M.L. 1973, A&A 26, 1
Lesh J.R., Aizenman M.L. 1978, ARA& A 16, 215
Napiwotzki R., Schönberner D., Wenske V. 1993, A&A 268, 653
North P., Rufener F., Figer A., Maurin L. 1981, Inf.Bull.Var.Stars No.2036
Osaki Y. 1971, PASJ 23, 485
Pearce J.A., Petrie R.M. 1951, Publ. Dominion Astrophys. Obs. 8, 409
Percy J.R. 1982, Inf.Bull.Var.Stars No.2085
Percy J.R., Madore K. 1971, in *New directions and New Frontiers in Variable Star Research*, Veröff. der Remeis-Sternwarte Bamberg 9, 197
Pigulski A., Boratyn D.A. 1992, A&A 253, 178

Plavec M. 1971, PASP 83, 144
Polfliet R., Smeyers P. 1990, A&A 237, 110
Poretti E. 1982, Inf.Bull.Var.Stars No.2239
Poretti E. 1984, Inf.Bull.Var.Stars No.2529
Simkin S.M. 1974, A&A 31, 129.
Slettebak A., Snow T.P. (Eds.) 1987, *Physics of Be Stars*, IAU Col. 92, Cambridge Univ. Press, Cambridge
Smak J. 1970, Acta Astron. 20, 75
Smith M.A. 1977, ApJ 215, 574
Smith M.A. 1978, ApJ 224, 927
Smith M.A. 1986, in *Hydrodymanic and Magnetohydrodynamic Problems in the Sun and Stars*, Ed. by Y. Osaki, Univ. of Tokyo, Tokyo, Japan, p. 145
Štefl S., Baade D., Harmanec P., Balona L.A. 1995, A&A 294, 135
Sterken C., Jerzykiewicz M. 1993, Space Sci. Rev. 62, 95
Stothers R., Simon N.R. 1969, ApJ 157, 673
Stothers R., Simon N.R. 1970, PASP 82, 707
Tarasov A.E., Harmanec P., Horn J., Lyubimkov L.S., Rostopchin S.I., Koubský P., Blake C., Kostunin V.V., Walker G.A.H., Yang S. 1995, A&AS 110, 59
Tassoul J.-L. 1987, ApJ 322, 856
Tassoul J.-L. 1988, ApJ 324, L71
Vidal C.R., Cooper J., Smith E.W. 1973, ApJS 25, 37
Waelkens C., Rufener F. 1983, A&A 121, 45
Walker G.A.H., Moyles K., Yang S., Fahlman G.G. 1982, PASP 94, 143
Walker G.A.H., Yang S., Fahlman G.G. 1979, ApJ 233, 199

This article was processed by the author using Springer-Verlag LaTeX A&A style file *L-AA* version 3.